中華民國建築學會「建築學報」第47期, PP.15~34, 2004年6月
Journal of Architecture, No. 47, PP.15~34, Jun. 2004

Strength and Flexural Rigidity of RC Columns under Biaxial Bending

Yun-Fei Chang * Yih-Houng Chen** Maw-Shyong Sheu***

Keywords: RC column; biaxial bending; flexural rigidity; full curve

ABSTRACT

This paper presents a rigorous method for performing the sectional analysis utilizing realistic stress-strain models for concrete and reinforcement, and a modification of the effective moment of inertia, I_e, in the current ACI Code to predict the load-deflection curves of RC columns under biaxial bending at any monotonic loading stage including post-ultimate stage. To verify the accuracy, forty experimental ultimate strength data are compared with the analytical results. Furthermore, three numerical examples are illustrated to provide design/check aids such as three-dimensional failure surfaces, interaction diagrams and dimensionless load contours. Seven experimental load-deflection curves are compared with the analytical results. It is observed that if some parameters are redefined, the effective moment of inertia, I_e, in the current ACI Code for flexural members can be employed to predict the complete load-deflection behavior very well.

雙軸彎曲鋼筋混凝土柱之強度與剛度分析

張雲妃* 陳義宏** 許茂雄***

關鍵字：鋼筋混凝土柱，雙軸彎曲，撓曲剛度，全程曲線

摘 要

根據「平面保持平面」與「應變諧合」之假設，本文在考慮鋼筋與混凝土材料受力破壞之上升段與下降段應力－應變全程曲線以及箍筋之圍束效應，利用簡單之靜力平衡條件，建立雙軸彎曲鋼筋混凝土柱斷面適用於任意載重階段之非線性聯立方程式，同時提出一簡單之演算法，處理圍束與非圍束並存以及異形斷面之數值求解方法。然後，改良現行規範之有效轉動慣量公式，使之適用於雙軸彎曲鋼筋混凝土柱上升段與下降段之載重－位移全程曲線。利用本文所發展之程式分析國內外四十支試驗柱之極限載重與七支試驗柱之載重－位移全程曲線，結果相當吻合，足以証明本文理論及演算法之準確性。最後，以常用三種斷面之設計輔助圖，提供雙軸彎曲RC柱實用分析資訊。

*成功大學建築學系博士候選人
* Ph. D. Candidate, Dept. of Architecture, National Cheng Kung University

**成功大學建築學系博士候選人
** Ph. D. Candidate, Dept. of Architecture, National Cheng Kung University

***成功大學建築學教授
***Professor, Dept. of Architecture, National Cheng Kung University

2004年3月16日受稿，2004年6月7日通過

I. INTRODUCTION

It is more difficult to predict the load-deflection curves for RC members than for structural steel members. This is mainly due to the nonlinearity of the materials, rigorous analysis for sections and the tension stiffening effect of concrete.

For material nonlinearity, Wegner (1978) pointed out that an improvement of the stress-strain relationship for reinforced concrete can increase the accuracy of the analytical results, sometimes more than that achieved using the finite element method. Furlong (1979) had the same observation in his research on biaxially loaded RC columns. Park *et al.* (1975) described more directly in their book that the parameters recommended for the equivalent concrete stress block are not applicable for columns with biaxial bending moments. Therefore, compared with other researches, the more realistic stress-strain models for concrete and reinforcement are utilized in this paper.

For rigorous section analysis, there is no exact analytical method to determine the strains and stresses in a nonhomogenous, anisotropic body with nonlinear material-behavior. Based on the Bernoulli hypothesis, a plane section before bending will remain plane after bending, a biaxially loaded RC column has three unknowns at each cross section. Theoretically, these three unknowns can be solved using the three simultaneous nonlinear equilibrium equations of force and moment. However, it seems to be very difficult and complex to solve the unknowns in closed form completely, if the realistic stress-strain material model, the irregularity of cross section and the reinforcement arrangement are taken into consideration simultaneously. Most researches usually made some simplified assumptions and/or used the finite element approach to overcome these difficulties. Actually, most biaxially loaded RC sections do not need to be analyzed using simplified assumptions or the time-consuming finite element approach. They can be analyzed by directly solving simultaneous nonlinear equilibrium equations of force and moment. Some researches have been carried out using the direct analysis approach for computing biaxiallly loaded column capacity (Dundar, 1990; Yen, 1991; Brøndum-Nielson, 1997; Rodriguez *et al.*, 1999). An equivalent rectangular concrete compressive stress block and perfectly elastoplastic reinforcement were usually used in these researches. This method cannot reflect the actual behavior. Therefore, the first purpose of this paper is to propose an accurate and direct analysis method for biaxially loaded RC sections utilizing the most realistic stress-strain models for the materials and integral methods to solve the three unknowns for such a column.

In order to calculate the deflection of the RC member, several countermeasures might be considered in the tension stiffening effect of the concrete. The simplest and most widely used countermeasure is implied in the 'effective moment inertia' calculation, which is assumed to be constant over the full length of the member. Several empirical expressions for the effective moment of inertia have been suggested (Branson, 1977; Sakai *et al.*, 1980; Branson *et al.*, 1982; Krishna Mohan Rao *et al.*, 1992), however, they are limited primarily to members subjected to uniaxial bending with/without axial force. Because most of the RC columns are subjected to axial force and biaxial bending under long-term and short-term loads, these problems have attracted considerable attention and several researches have been made in the past few years. While most of these researches devel-

oped an approximate analysis method, design aids (Furlong, 1961; Taylor, 1985; Hsu, 1988) or utilized the finite segment approach to analyze the load-deflection curves (Wang *et al.*, 1992), few researches so far have focused on the flexural rigidity of biaxially loaded RC columns. All of these researches were concerned with the flexural rigidity of slender RC columns at buckling or yielding load (Furlong, 1979; Resheidat *et al.*, 1996). This approach is used in the current *ACI* Code (1999) for moment magnifier, not for calculating or tracing load-deflection curves. It seems that there is no research that has ever attempted to investigate the 'effective moment of inertia' to predict the load-deflection curves of biaxially loaded RC columns. Accordingly, the second purpose of this paper is to propose a reasonable 'effective moment inertia' to accurately predict the load-deflection curves of biaxially loaded RC columns.

II. BASIC ASSUMPTIONS

The following assumptions are made in this paper:

1. Based on the Bernoulli hypothesis, the cross section remains plane and normal to the deflection line.
2. Shear deformations are neglected.
3. The tensile strength of concrete is neglected in the section analysis.

III. STRESS-STRAIN MODELS OF MATERIALS

This paper utilizes realistic stress-strain models for concrete and reinforcement. With the strain and stress in compression positive, the mathematical formulas for such models are as follows:

1. Concrete

The modified Kent and Park models (Park *et al.*, 1982) for both confined and unconfined concrete are used in this study, as shown in Fig. 1:

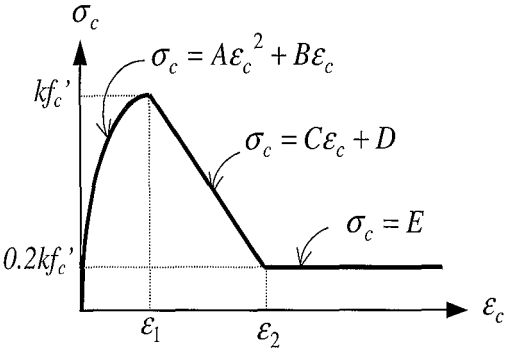

Fig. 1. Stress-strain curves for confined and unconfined concrete

$$\sigma_c = 0 \quad ; \ \varepsilon_c < 0 \tag{1a}$$

$$\sigma_c = A\varepsilon_c^{\,2} + B\varepsilon_c \quad ; \ 0 \le \varepsilon_c < \varepsilon_1 \tag{1b}$$

$$\sigma_c = C\varepsilon_c + D \quad ; \ \varepsilon_1 \le \varepsilon_c < \varepsilon_2 \tag{1c}$$

$$\sigma_c = E \quad ; \ \varepsilon_2 \le \varepsilon_c \tag{1d}$$

in which

$$A = -kf_c'/(k\varepsilon_o)^2$$

$$B = 2f_c'/\varepsilon_o$$

$$C = -0.5kf_c'/(\varepsilon_{50u} + \varepsilon_{50h} - k\varepsilon_o)$$

$$D = kf'[1 + 0.5k\varepsilon_o/(\varepsilon_{50u} + \varepsilon_{50h} - k\varepsilon_o)]$$

$$E = 0.2kf_c'$$

$$\varepsilon_1 = k\varepsilon_o,$$

$$\varepsilon_2 = k\varepsilon_o + 1.6(\varepsilon_{50u} + \varepsilon_{50h} - k\varepsilon_o)$$

σ_c and ε_c denote the stress and strain of concrete, respectively. f_c' denotes the specified compressive strength of concrete and k, ε_o, ε_{50u}, ε_{50h} are defined in detail in (Park *et al.*, 1982). Setting different values for ε_1, ε_2 and parameters A~E, Eqs. (1) are identical to those for other models, such as the Modified Hognestad model:

$$A = -f_c' / \varepsilon_o^2$$
$$C = -0.15 f_c' / (\varepsilon_2 - \varepsilon_1)$$
$$D = f_c'(\varepsilon_2 - 0.85\varepsilon_1) / (\varepsilon_2 - \varepsilon_1)$$
$$E = 0$$
$$\varepsilon_1 = 1.8 f_c' / E_c, \quad \varepsilon_2 = 0.0038$$

and parabola-rectangular model:

$$A = -f_c' / \varepsilon_o^2, \quad C = 0$$
$$D = 0.85 f_c', \quad E = 0$$
$$\varepsilon_1 = 0.002 \text{ or } 1.6 f_c' / E_c$$
$$\varepsilon_2 = 0.0035$$

2. Reinforcement

The reinforcement formulas are derived from Fig. 2:

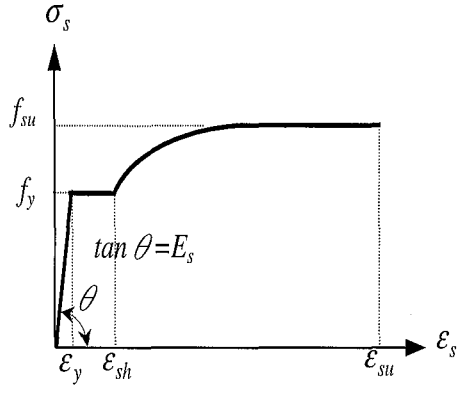

Fig. 2. Stress-strain curve for reinforcement in tension or compression

$$\sigma_s = E_s \varepsilon_s \quad ; \ 0 \le |\varepsilon_s| < \varepsilon_y \tag{2a}$$

$$\sigma_s = f_y \frac{\varepsilon_s}{|\varepsilon_s|} \quad ; \ \varepsilon_y \le |\varepsilon_s| < \varepsilon_{sh} \tag{2b}$$

$$\sigma_s = \left\{ (f_y - f_{su})[(\varepsilon_s - \varepsilon_{su})/(\varepsilon_{sh} - \varepsilon_{su})]^2 + f_{su} \right\} \frac{\varepsilon_s}{|\varepsilon_s|} \ ;$$
$$\varepsilon_{sh} \le |\varepsilon_s| < \varepsilon_{su} \tag{2c}$$

in which σ_s and ε_s denote the stress and strain of reinforcement, E_s, f_y, f_{su}, ε_y, ε_{sh}, and ε_{su} denote the modulus of elasticity, yielding strength, ultimate strength, yielding strain, hardening strain, and ultimate strain of reinforcement, respectively. Setting $f_{su} = f_y$, the presented model is identical to the perfectly elastoplastic model.

IV. SECTION ANALYSIS

Based on the basic principles of equilibrium, compatibility, and superposition, the analysis method for biaxially loaded RC sections is presented.

1. Derivation of Nonlinear Equilibrium Equations

Here equations for a partially-cracked rectangular section with fully-confined or fully-unconfined concrete are derived. Refer to Fig. 3, considering a partially-cracked rectangular column cross-section with width b and height d subjected to load P at coordinate (x_p, y_p) in the X-Y coordinates. P is taken as positive when compressive. Let Y' be the neutral axis that intersects the X-axis and Y-axis at a and h, respectively. The depth of the neutral axis, kd, is

$$kd = ah / \sqrt{a^2 + h^2} \tag{3}$$

X' is perpendicular to Y' and passing through the tip of the corner. For convenience, since this section should bend about Y'(neutral axis), the equations will be derived with respect to the load-depended X' –Y' coordinates. The transformation between X–Y and X' –Y' are

$$x' = kd\left(1 - a^{-1}x - h^{-1}y\right) \tag{4a}$$

$$y' = kd\left(h^{-1}x - a^{-1}y\right) \tag{4b}$$

From the free body equilibrium, we have $\Sigma F = 0$, $\Sigma M_{X'} = 0$ and $\Sigma M_{Y'} = 0$. That is:

$$\int \sigma_c dA_c + \sum_{i=1}^{NS} (\sigma_{si} - \sigma_{ci}) A_{si} - P = 0 \quad (5a)$$

$$\int x' \sigma_c dA_c + \sum_{i=1}^{NS} x'_{si} (\sigma_{si} - \sigma_{ci}) A_{si} - P x'_p = 0 \quad (5b)$$

$$\int y' \sigma_c dA_c + \sum_{i=1}^{NS} y'_{si} (\sigma_{si} - \sigma_{ci}) A_{si} - P y'_p = 0 \quad (5c)$$

where NS is the total number of reinforcement. A_{si} is the cross-sectional area of reinforcement i. σ_{si} is the reinforcement i stress. σ_{ci} is the concrete stress at the position of reinforcement i. (x'_{si}, y'_{si}) and (x'_p, y'_p) are the coordinates for the reinforcement i and load P in the X'–Y' coordinates, respectively. Since the location of the neutral axis is unknown, it is difficult to carry out the integral of Eqs. (5). In order to simplify the expression of Eqs.(5), the following parameters are defined :

$$\alpha_o = \left(1 - ba^{-1}\right) \geq 0 \quad (6a)$$

$$\alpha_1 = \left[\left(\gamma_o - ba^{-1}\right) / \left(1 - ba^{-1}\right)\right] \geq 0 \quad (6b)$$

$$\beta_o = \left(1 - dh^{-1}\right) \geq 0 \quad (6c)$$

$$\beta_1 = \left[\left(\gamma_o - dh^{-1}\right) / \left(1 - dh^{-1}\right)\right] \geq 0 \quad (6d)$$

$$\gamma_o = \left(1 - \varepsilon_1 \varepsilon_{co}^{-1}\right) \geq 0 \quad (6e)$$

$$\gamma_1 = \left(1 - \varepsilon_2 \varepsilon_{co}^{-1}\right) \geq 0 \quad (6f)$$

in which $\geq$ denotes that zero is substituted for the negative value. Suppose that the maximum concrete compressive strain at the tip of the corner is ε_{co}, and let a, h and ε_{co} be the unknowns for the section. Expanding Eqs. (5) and introducing Eqs. (6), we acquire the simultaneous nonlinear equilibrium equations for the section as shown in Fig. 3:

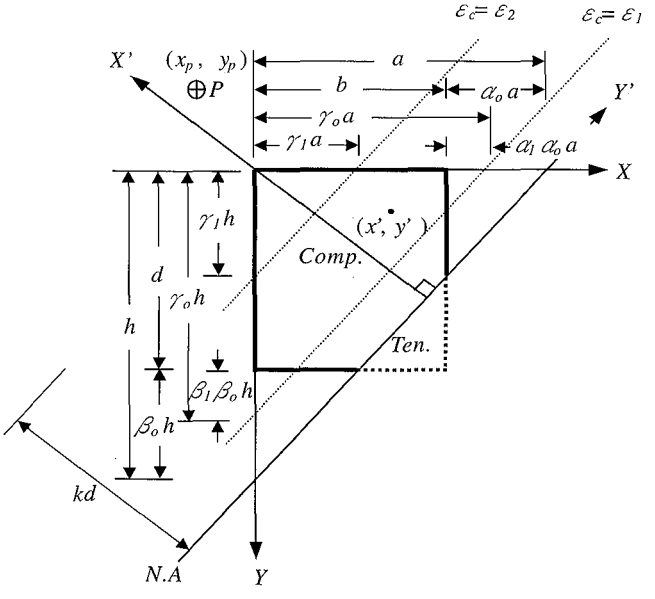

Fig. 3. Geometry under biaxial bending and axial load

$$ah/12\left(k_1\varepsilon_{co}{}^2+k_2\varepsilon_{co}+k_3\right)+\sum_{i=1}^{NS}\left(\sigma_{si}-\sigma_{ci}\right)A_{si}-P=0 \tag{7a}$$

$$ah/60\left(k_4\varepsilon_{co}{}^2+k_5\varepsilon_{co}+k_6\right)+\sqrt{a^2+h^2}/a/h\sum_{i=1}^{NS}x'_{si}\left(\sigma_{si}-\sigma_{ci}\right)A_{si}$$
$$-P\left(1-a^{-1}x_p-h^{-1}y_p\right)=0 \tag{7b}$$

$$1/120\left[\left(k_7a^2+k_8h^2\right)\varepsilon_{co}{}^2+\left(k_9a^2+k_{10}h^2\right)\varepsilon_{co}+k_{11}a^2+k_{12}h^2\right]$$
$$+\sqrt{a^2+h^2}/a/h\sum_{i=1}^{NS}y'_{si}\left(\sigma_{si}-\sigma_{ci}\right)A_{si}-P\left(h^{-1}x_p-a^{-1}y_p\right)=0 \tag{7c}$$

where $k_1 \sim k_{12}$

$$k_1=A\left[1-\alpha_o{}^4-\beta_o{}^4-\gamma_o{}^2\left(3\gamma_o{}^2-8\gamma_o+6\right)+\alpha_o{}^4\alpha_1{}^2\left(3\alpha_1{}^2-8\alpha_1+6\right)+\beta_o{}^4\beta_1{}^2\left(3\beta_1{}^2-8\beta_1+6\right)\right] \tag{8a}$$

$$k_2=2\left\{B\left(1-\alpha_o{}^3-\beta_o{}^3\right)+(C-B)\left[\gamma_o{}^2(3-2\gamma_o)-\alpha_o{}^3\alpha_1{}^2(3-2\alpha_1)-\beta_o{}^3\beta_1{}^2(3-2\beta_1)\right]\right.$$
$$\left.-C\gamma_1{}^2(3-2\gamma_1)\right\} \tag{8b}$$

$$k_3=6\left\{D\left(\gamma_o{}^2-\alpha_o{}^2\alpha_1{}^2-\beta_o{}^2\beta_1{}^2\right)+(E-D)\gamma_1{}^2\right\} \tag{8c}$$

$$k_4=3A\left[1-\alpha_o{}^5-\beta_o{}^5-\gamma_o{}^2\left(10-20\gamma_o+15\gamma_o{}^2-4\gamma_o{}^3\right)+\alpha_o{}^5\alpha_1{}^2\left(10-20\alpha_1+15\alpha_1{}^2-4\alpha_1{}^3\right)\right.$$
$$\left.+\beta_o{}^5\beta_1{}^2\left(10-20\beta_1+15\beta_1{}^2-4\beta_1{}^3\right)\right] \tag{8d}$$

$$k_5=5\left\{B\left(1-\alpha_o{}^4-\beta_o{}^4\right)+(C-B)\left[\gamma_o{}^2\left(3\gamma_o{}^2-8\gamma_o+6\right)-\alpha_o{}^4\alpha_1{}^2\left(3\alpha_1{}^2-8\alpha_1+6\right)\right.\right.$$
$$\left.\left.-\beta_o{}^4\beta_1{}^2\left(3\beta_1{}^2-8\beta_1+6\right)\right]-C\gamma_1{}^2\left(3\gamma_1{}^2-8\gamma_1+6\right)\right\} \tag{8e}$$

$$k_6=10\left\{D\left[\gamma_o{}^2(3-2\gamma_o)-\alpha_o{}^3\alpha_1{}^2(3-2\alpha_1)-\beta_o{}^3\beta_1{}^2(3-2\beta_1)\right]+(E-D)\gamma_1{}^2(3-2\gamma_1)\right\} \tag{8f}$$

$$k_7=2A\left[1+4\alpha_o{}^5-5\alpha_o{}^4-\beta_o{}^5-\gamma_o{}^3\left(6\gamma_o{}^2-15\gamma_o+10\right)+\alpha_o{}^5\alpha_1{}^3\left(6\alpha_1{}^2-15\alpha_1+10\right)\right.$$
$$\left.+\beta_o{}^5\beta_1{}^3\left(6\beta_1{}^2-15\beta_1+10\right)+5\alpha_o{}^4\alpha_1{}^2\left(3\alpha_1{}^2-8\alpha_1+6\right)\left(\gamma_o-\alpha_o\alpha_1\right)\right] \tag{8g}$$

$$k_8 = -2A\left[1+4\beta_o^5-5\beta_o^4-\alpha_o^5-\gamma_o^3\left(6\gamma_o^2-15\gamma_o+10\right)+\alpha_o^5\alpha_1^3\left(6\alpha_1^2-15\alpha_1+10\right)\right.$$
$$\left.+\beta_o^5\beta_1^3\left(6\beta_1^2-15\beta_1+10\right)+5\beta_o^4\beta_1^2\left(3\beta_1^2-8\beta_1+6\right)\left(\gamma_o-\beta_o\beta_1\right)\right] \quad 8(h)$$

$$k_9 = 5\left\{B\left(1+3\alpha_o^4-4\alpha_o^3-\beta_o^4\right)+(C-B)\left[\gamma_o^3(4-3\gamma_o)-\alpha_o^4\alpha_1^3(4-3\alpha_1)-\beta_o^4\beta_1^3(4-3\beta_1)\right.\right.$$
$$\left.\left.-4\alpha_o^3\alpha_1^2(3-2\alpha_1)(\gamma_o-\alpha_o\alpha_1)\right]-C\gamma_1^3(4-3\gamma_1)\right\} \quad 8(i)$$

$$k_{10} = -5\left\{B\left(1+3\beta_o^4-4\beta_o^3-\alpha_o^4\right)+(C-B)\left[\gamma_o^3(4-3\gamma_o)-\alpha_o^4\alpha_1^3(4-3\alpha_1)-\beta_o^4\beta_1^3(4-3\beta_1)\right.\right.$$
$$\left.\left.-4\beta_o^3\beta_1^2(3-2\beta_1)(\gamma_o-\beta_o\beta_1)\right]-C\gamma_1^3(4-3\gamma_1)\right\} \quad 8(j)$$

$$k_{11} = 20\left\{D\left[\gamma_o^3-\alpha_o^3\alpha_1^3-\beta_o^3\beta_1^3-3\alpha_o^2\alpha_1^2(\gamma_o-\alpha_o\alpha_1)\right]+(E-D)\gamma_1^3\right\} \quad 8(k)$$

$$k_{12} = -20\left\{D\left[\gamma_o^3-\alpha_o^3\alpha_1^3-\beta_o^3\beta_1^3-3\beta_o^2\beta_1^2(\gamma_o-\beta_o\beta_1)\right]+(E-D)\gamma_1^3\right\} \quad 8(l)$$

2. Extended application of Equations

Eqs. (7) are derived from a partially-cracked rectangular cross section with fully-confined or fully-unconfined concrete. However, based on the algorithms shown in Fig. 4, Eqs. (7) can be applied to analyze some types of biaxially loaded RC sections, such as fully-uncracked, partially-confined, channel-shaped, L-shaped, and rectangular hollow-shaped cross sections etc.

3. Solution of simultaneous nonlinear Equilibrium Equations

A FORTRAN 90 module, based on Broyden's method and line search procedure, was written to solve simultaneous nonlinear equations. The details of this method are far beyond the scope of this paper. Because an extensive explanation of this technique has been published in many numerical textbooks (William *et al.*, 1994), it is not described herein.

4. Comparison with Experiment Results

In order to check the accuracy of the method and computer program developed in this paper, forty experimental specimens by other researches (Bresler, 1960; Ramamurthy, 1966; Hsu, 1974; Heimdahl *et al.*, 1975) were analyzed for comparison of the ultimate load P_u. To calculate maximum eccentric load P_u, the three unknowns in Eqs. (7) were changed to P, a and h. Let the maximum concrete tip strain ε_{co} be given and increase from zero to whichever corresponding P is less than the latest one. For each given ε_{co}, we can acquire the corresponding P, a and h. The maximum value for the series output P is the ultimate capacity that the column can be subjected. The hoop confinement effects are considered, i.e. the column sec-

tion is divided into a confined concrete core and an unconfined concrete cover. The principle of superposition, as shown in Fig. 4(b), is then applied. The analytical and experimental results, which show excellent agreement, are listed in Table 1. The maximum and average absolute errors are 9.7% and 3.9%, respectively.

V. APPLICATION EXAMPLES

The verified computer program developed in this paper can also be applied to generate design/check aids for biaxial bending with/without an axial load, such as three-dimensional failure surfaces, interaction diagrams and dimensionless load contours. There are three examples for rectangular solid, rectangular hollow, and L-shaped sections presented herein.

Although the realistic stress-strain curves for concrete and rebars and the confinement effects of hoops can be taken into consideration, the following assumptions are made just for design purposes:

1. The maximum compressive strain of concrete is 0.003.
2. The stress-strain curve for rebars is perfectly elasto-plastic.
3. The confinement effects of hoops and bukling of longitudinal rebars are not taken into consideration.

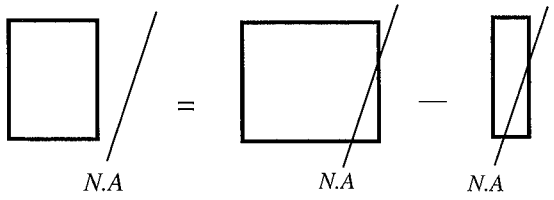

(a) Fully-uncracked section

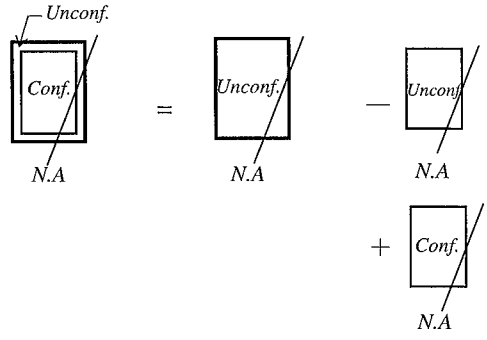

(b) Partially-confined section

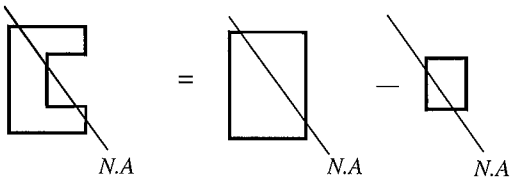

(c) Channel-shaped section

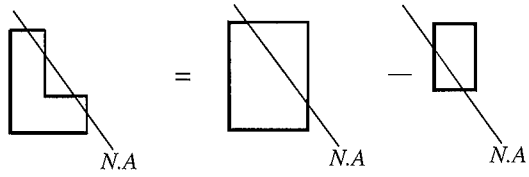

(d) L-shaped section

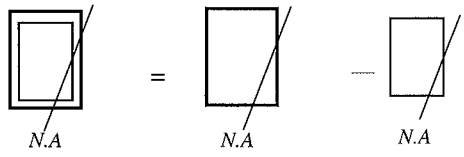

(e) Rectangular hollow-shaped section

Comp. Ten.

Fig. 4. Utilization of superposition

Table 1. Comparison of ultimate loads

Reference	Specimen No.	e_x (cm)	e_y (cm)	P_u (kN)			ε_{co} (10^{-3})	Error (%)
				Tested	Calculated by reference	Calculated by this paper		
Bresler (1960)	B-5	7.62	10.16	142	157	156	4.0	9.7
	B-6	15.24	20.32	75	63	74	3.4	-2.6
	B-7	15.24	10.16	93	83	97	5.0	4.2
	B-8	7.62	20.32	107	96	108	4.4	0.9
Ramamurthy (1966)	A-15	3.54	3.54	267	–	267	4.0	0.0
	B-1	2.10	7.85	629	614	628	3.6	-0.2
	B-2	1.94	4.69	772	787	806	3.6	4.3
	B-3	5.10	8.80	534	526	518	4.0	-2.9
	B-4	6.40	11.00	396	409	404	4.0	2.0
	B-6	6.47	6.47	501	512	513	4.0	2.3
	B-7	7.18	7.18	516	487	484	4.0	-6.3
	B-8	10.16	10.16	369	338	356	3.6	-3.7
	D-1	2.54	3.80	787	794	797	3.6	1.2
	D-2	5.57	8.45	401	394	392	4.4	-2.2
	D-3	7.62	11.41	312	290	291	4.6	-6.6
	D-4	3.23	3.23	681	653	687	4.0	-0.9
	D-5	8.08	8.08	378	345	346	4.0	-8.5
	D-6	7.92	4.57	401	408	374	4.4	-6.6
	E-1	6.01	11.40	465	447	419	4.2	-9.7
	E-2	7.62	15.24	312	314	310	4.6	-0.6
	E-4	6.60	3.81	543	576	543	4.2	0.0
Heimdahi & Bianchini (1975)	ER-1	6.36	2.63	187	141	172	5.0	-7.9
	ER-2	12.42	5.14	82	75	87	4.6	6.0
	FR-1	4.87	4.87	170	138	167	4.8	-1.7
	FR-2	8.06	8.06	81	73	83	4.6	2.4
	EW-1	6.40	2.65	172	138	157	5.0	-9.1
	EW-2	12.46	5.16	76	73	80	5.6	5.1
	FW-1	4.84	4.84	162	136	152	4.8	-6.1
	FW-2	9.50	9.50	72	71	76	5.4	6.8
Hsu (1974)	H-1	7.62	5.08	62	60	62	4.6	0.0
	H-2	8.26	5.72	53	57	58	4.2	9.3
	H-3	6.35	7.62	61	60	60	4.2	-1.6
	S-1	2.54	3.81	93	96	98	3.4	5.3
	S-2	2.54	3.81	110	111	110	3.2	0.0
	U-1	6.35	8.89	43	44	43	4.8	0.0
	U-2	7.62	8.89	39	40	40	5.0	2.5
	U-3	8.89	8.89	35	37	37	5.0	5.6
	U-4	5.08	5.08	64	67	66	4.8	3.1
	U-5	1.27	10.16	48	46	51	4.8	6.1
	U-6	1.27	17.78	27	27	27	3.4	0.0
						Maximum absolute error		9.7
						Average absolute error		3.9

Note: e_x = eccentricity of axial load along X-axis

e_y = eccentricity of axial load along Y-axis

Instead of varying the angle or location of the assumed neutral axis (Furlong, 1961; Taylor, 1985), the triplets (P_n, M_{nx}, M_{ny}) on the failure surface of a given section are generated by varying the loading axis angle θ under a series of constant axial loads P_n at the plastic centroid of the section. This solution strategy is good because the triplets can be obtained directly using the real loading axis angle and not by interpolation between the two nearest curves produced by the predetermined neutral axis. This is more precise, convenient and faster.

The dimension and material properties of these examples are shown in detail in Figs. 5(a), 6 (a) and 7(a). The analytical results are shown in Figs. 5(b)~(e), 6(b)~(e) and 7(b)~(f), in which P_o is nominal axial load strength at zero eccentricity. It must be emphasized again that the intersected points on the failure surfaces are the direct analytical results, not interpolated or extrapolated by some powerful graphic program. They are smooth enough to prove the reliability and accuracy of the algorithm presented in this paper.

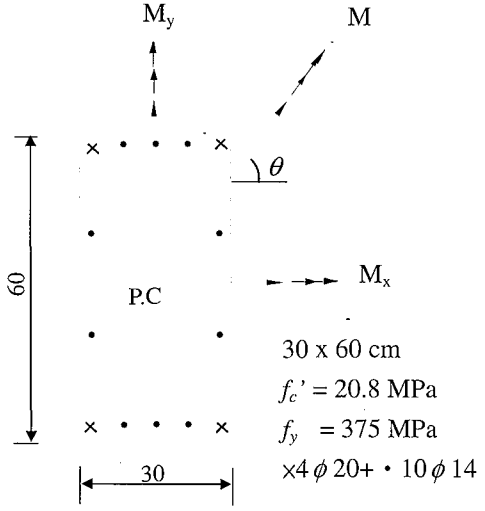

(a)Section details

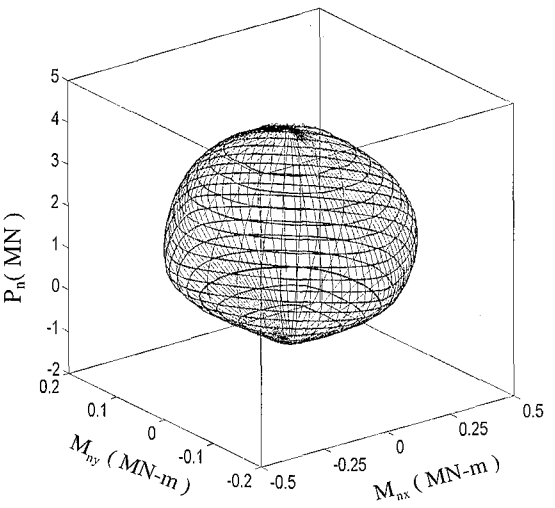

(b) Failure surface

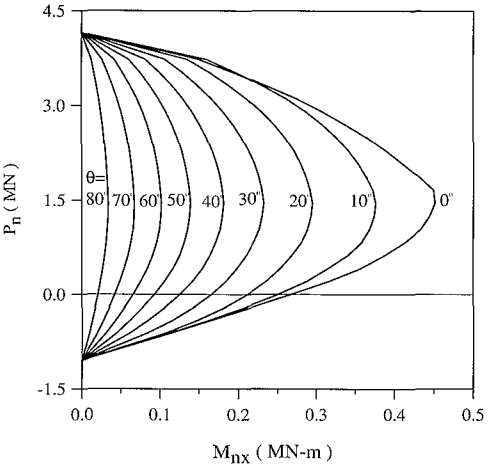

(c) Quadrantal interaction Diagram

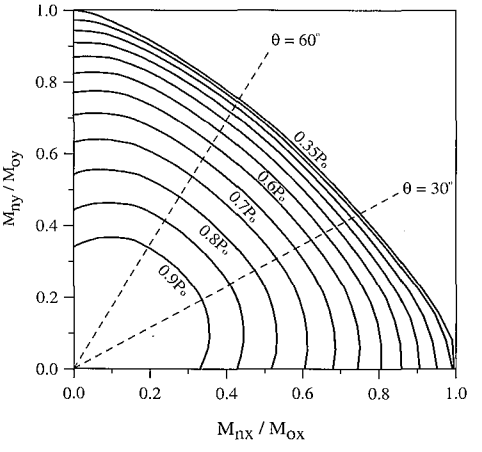

(d) Quadrantal top view of failure surface

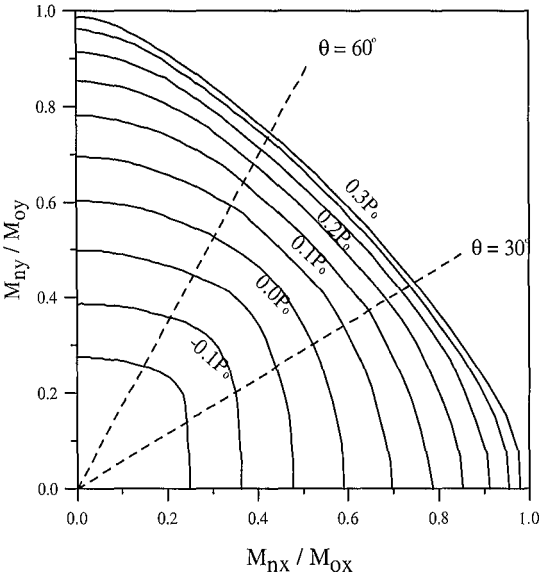

(e) Quadrantal bottom view of failure surface

Fig. 5. Rectangular solid section

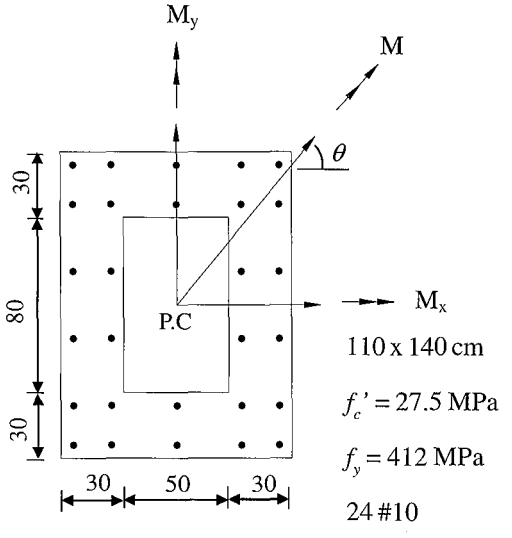

(a) Section details

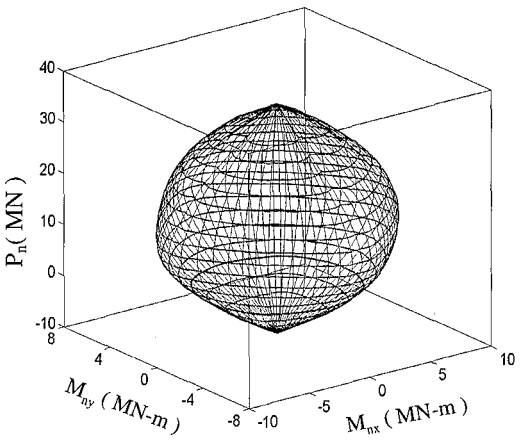

(b) Failure surface

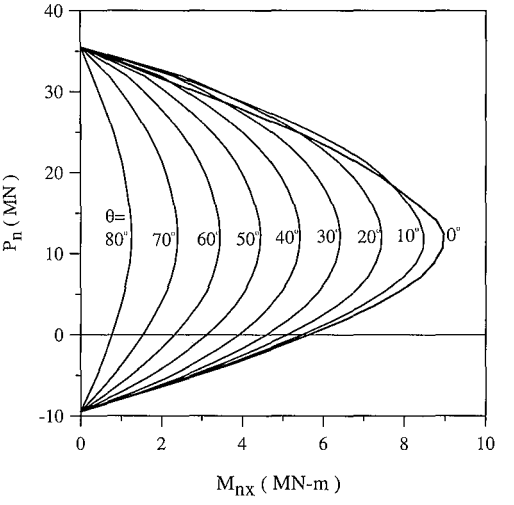

(c) Quadrantal interaction diagram

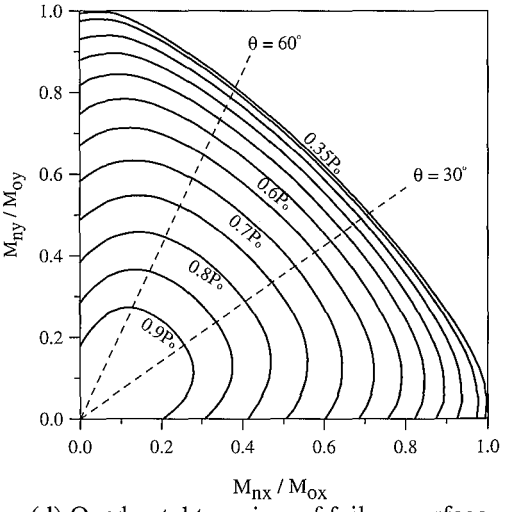

(d) Quadrantal top view of failure surface

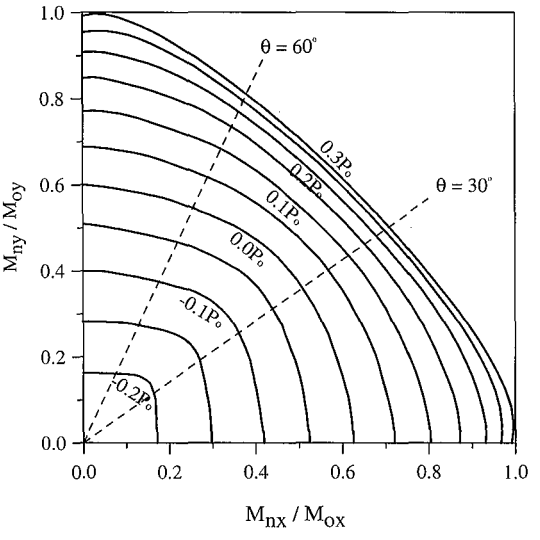

(e) Quadrantal bottom view of failure surface

Fig. 6. Rectangular hollow section

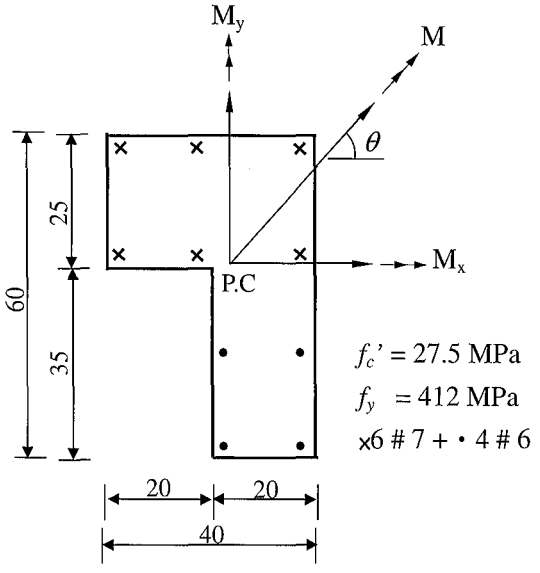

(a) Section details

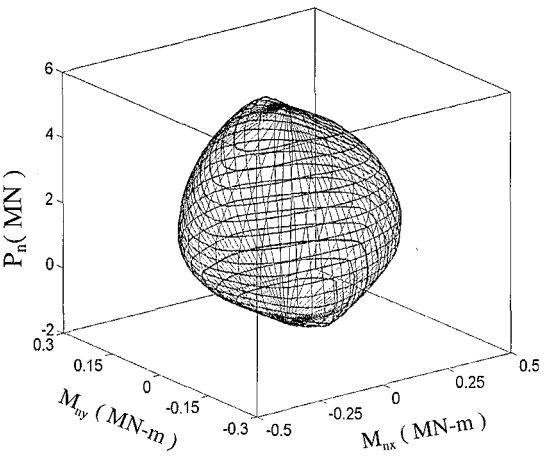

(b) Failure surface

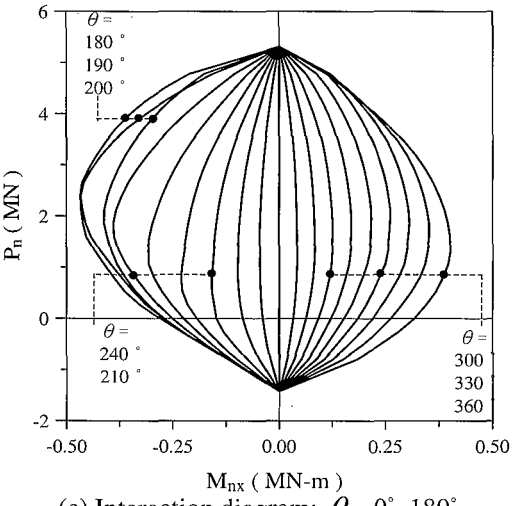

(c) Interaction diagram: θ =0°~180°

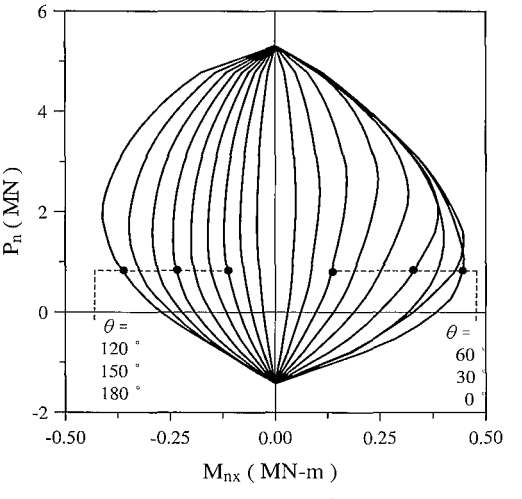

(d) Interaction diagram: θ =180°~360°

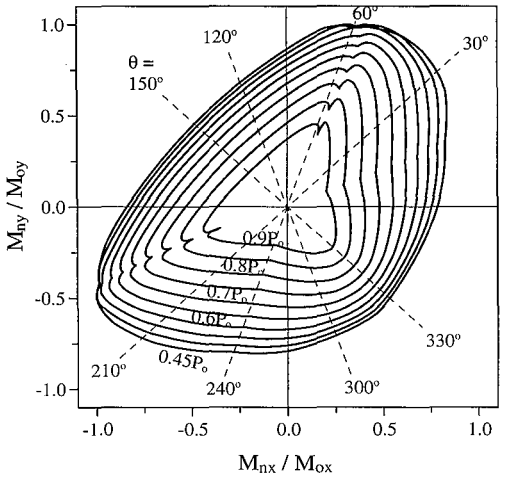

(e)Top view of failure surface

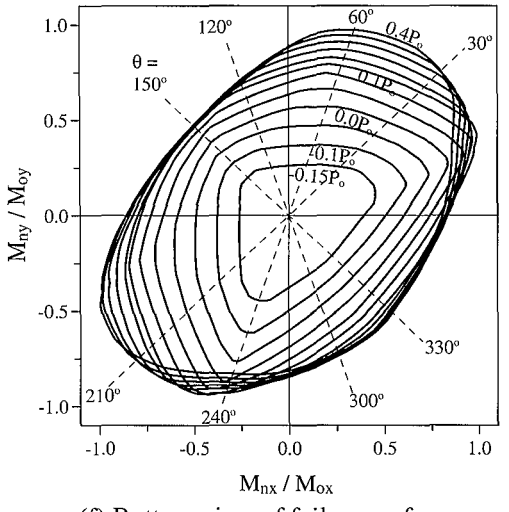

(f) Bottom view of failure surface

Fig. 7. L-shaped section

VI. EFFECTIVE FLEXURAL RIGIDITY

The effective flexural rigidity E_cI_e is the product of two quantities E_c and I_e, in which E_c is the modulus of elasticity of concrete defined by the *ACI* Code, and I_e is effective moment of inertia. Over the past few years, several empirical equations for I_e have been suggested. The best-known and most widely used equation was proposed by Branson (1977) and adopted by the current *ACI* Code for members subjected to uniaxial bending without an axial load. For members subjected to uniaxial bending and axial force, Branson *et al.* (1982) proposed a modification for M_{cr} in his formula. However, this is not applicable to the post-ultimate stage because I_e does not decrease with softening.

Theoretically, the section should bend about an instantaneous neutral axis. In other words, the E_cI_e calculation for biaxially loaded columns may be simplified into that for uniaxially loaded columns. Accordingly, I_e is proposed as:

$$I_e = \left(\frac{M_{cr}}{M_{\max}}\right)^3 I_{gt} + \left[1 - \left(\frac{M_{cr}}{M_{\max}}\right)^3\right] I_{cr} \quad \text{.....(9)}$$

in which

I_{gt} = moment of inertia of the uncracked transformed section, with respect to the axis that passes through the centroid and parallel to the instantaneous neutral axis of the section

I_{cr} = moment of inertia of the cracked transformed section, with respect to the axis that passes through the centroid and parallel to the instantaneous neutral axis of the section.

M_{max} = maximum moment in the member, with respect to the instantaneous neutral axis

$M_{cr} = (f_r + P/A_g)\, I_{gt} / y_t$, cracking moment associated with I_{gt}

f_r = $0.7\sqrt{f_c'}$, MPa, modulus of rupture of concrete

y_t = distance from the reference axis of I_{gt} to extreme fiber in tension

P and A_g are normal force and gross area of section, respectively.

To reflect the realistic behavior of the material, the modulus of elasticity of concrete is different strip by strip, therefore the mechanical characteristics of concrete are calculated strip by strip. In general, 100 strips give sufficient accuracy for sectional analysis. In order to calculate I_{cr}, the area of discrete concrete strips and reinforcement is transformed into unstressed plain concrete area using the ratio E_c^{sec}/E_c and E_s^{sec}/E_c, in which E_c^{sec} and E_s^{sec} are the secant modulus of elasticity at a specific local strain in each concrete strip and reinforcement, respectively, as shown in Fig. 8. Thus, I_{cr} is not constant and decreasing with the maximum concrete compressive strain of the section increasing.

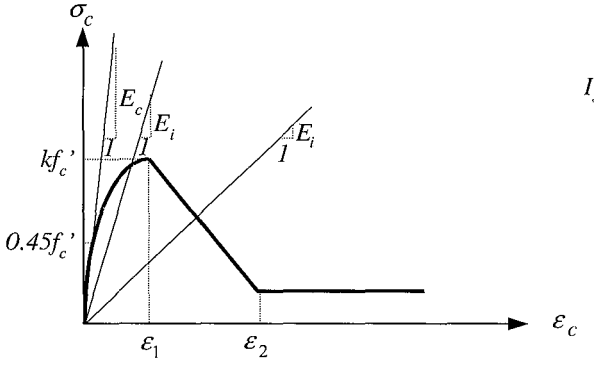

(a) Concrete

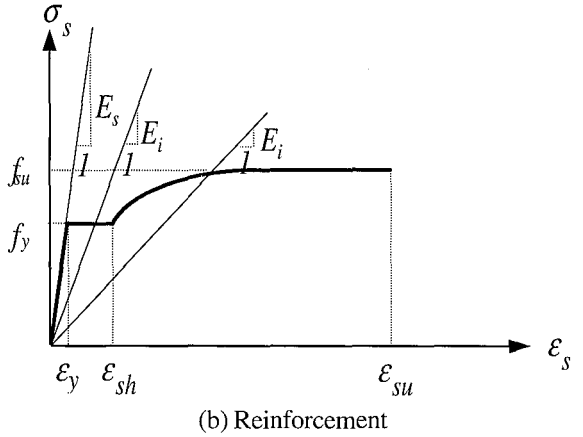

(b) Reinforcement

Fig. 8. Secant modulus of elasticity

Furthermore, special emphasis is placed on M_{max}, especially in the post-ultimate stage. In the pre-ultimate stage, M_{max} is essentially identical to that in the *ACI* Code. While in the post-ultimate stage, the ultimate bending capacity of the column, M_u, is substituted for M_{max}. This is reasonable because the curvature localization phenomena appears at the peak load. Thereafter deflection depends tremendously on I_{cr} of the section. Mathematically, Eq. (9) is an interpolation function of the upper bond I_{gt} and lower bond I_{cr}. Utilizing M_u in this equation, leads I_e to remain close to I_{cr}, as shown in Fig. 9. Therefore, it is reasonable to reflect on the curvature localization phenomena in the post-ultimate stage.

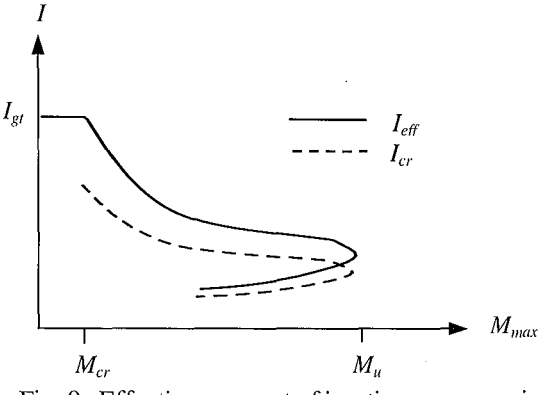

Fig. 9. Effective moment of inertia versus maximum moment

Comparison with Experimental Results

Seven test specimens from two researches (Tsao, 1991; Liu, 1997) are analyzed to compare the monotonic eccentric load-lateral deflection curves. All specimens were loaded eccentrically and the details are shown in Table 2 and Fig. 10. The flow Chart for the load-deflection curve calculation is shown in Fig. 11. The load controls it when the maximum concrete compressive strain, ε_{co}, is less than 0.003. Otherwise, the maximum concrete compressive strain, ε_{co}, controls it. The following assumptions are made:

1. To model the true behavior of concrete spalling, let E=0 in Eq. (1d) to restrict $\sigma_c = 0$ when $\varepsilon_c \geq \varepsilon_2$.
2. The P–Δ secondary effect is taken into consideration, where Δ is the latest lateral deflection.
3. The brackets at both ends must be rigid enough to prevent cracking, i.e. the flexural rigidity remains constant. Therefore, the specimens can be considered as pin-ended columns with stepped sections. The lateral deflection calculation is carried out using the conjugate-beam method and the effective moment of inertia formula, Eq. (9), in this paper.

Figures 12 and 13 show the comparison between experimental and analytical curves. They are reasonably matched even in the failure stage.

Table 2. Details of specimens

Reference	Specimen No.	L (cm)	L' (cm)	f_c' (MPa)	f_y (MPa)	Rebar reinforcement	Space of hoop (cm)	e_x (cm)	e_y (cm)
Liu (1997)	M03	175.0	20.0	31.5	470.9	4-#4	10.0	10.6	10.6
	M04	175.0	20.0	25.9	470.9	4-#4	12.5	10.6	10.6
	M08	175.0	20.0	21.6	470.9	4-#4	15.0	10.6	10.6
	C18	175.0	20.0	29.4	470.9 , 467.6	4-#4, 4-#3	10.0	10.6	10.6
Tsao (1991)	C1	121.9	20.3	19.1	544.4	4-#3	7.62	0.97	2.35
	C5	121.9	20.3	25.5	420.3	4-#3	7.62	1.94	4.69
	C6	121.9	20.3	25.5	420.3	4-#3	7.62	0.97	2.35

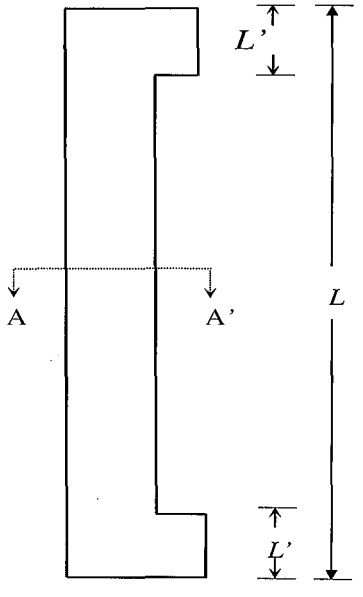

(a) Elevation

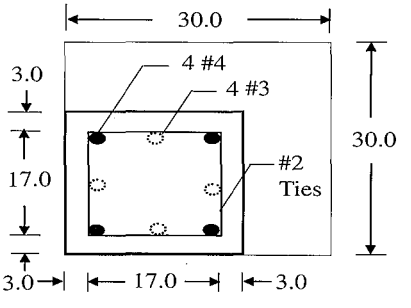

(b) Section A-A', Liu (1997)

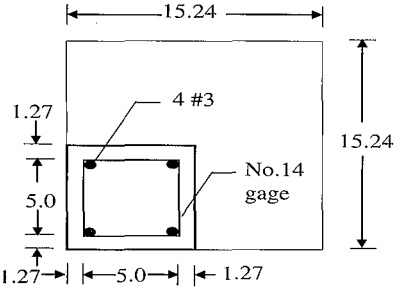

(c) Section A-A', Tsao (1991)

Fig. 10. Specimen elevation and sections (dimension in cm)

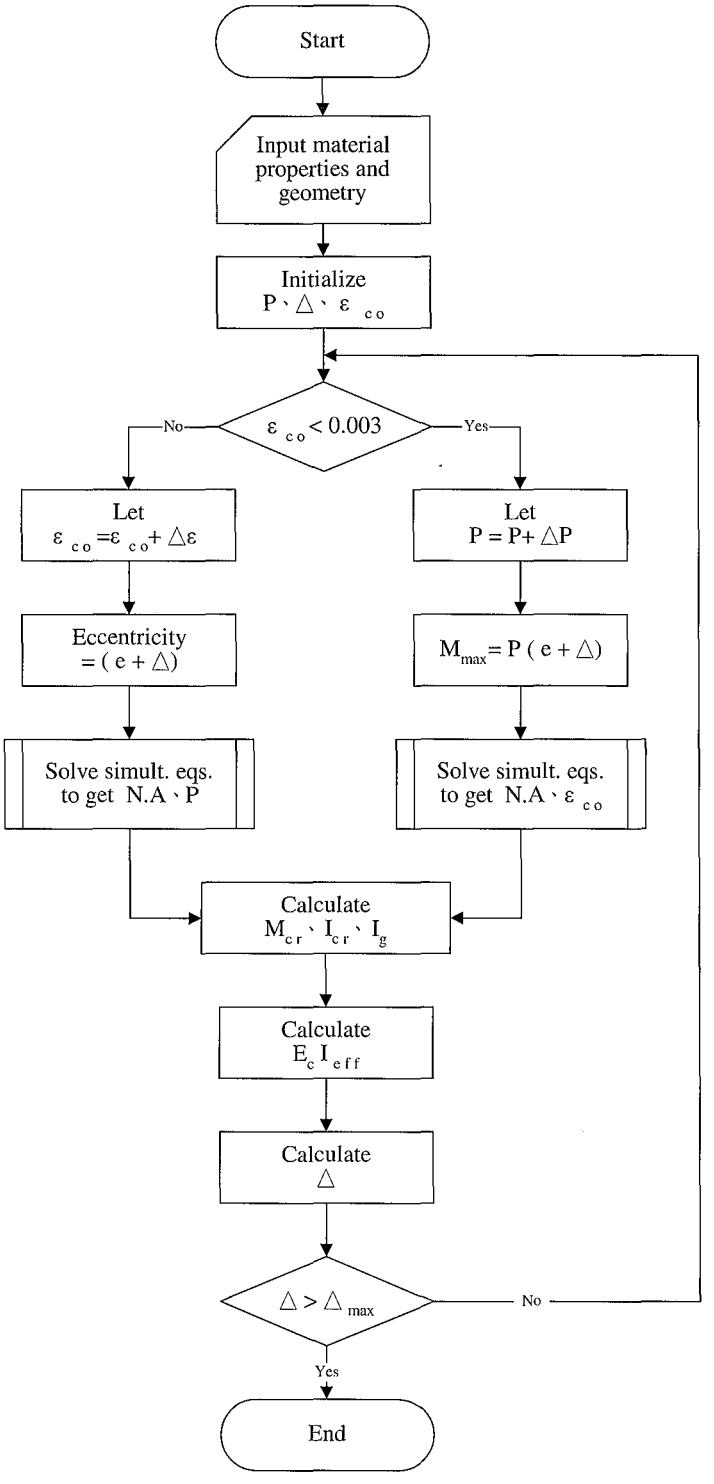

Fig. 11. Flow chart for the load-deflection curve calculation

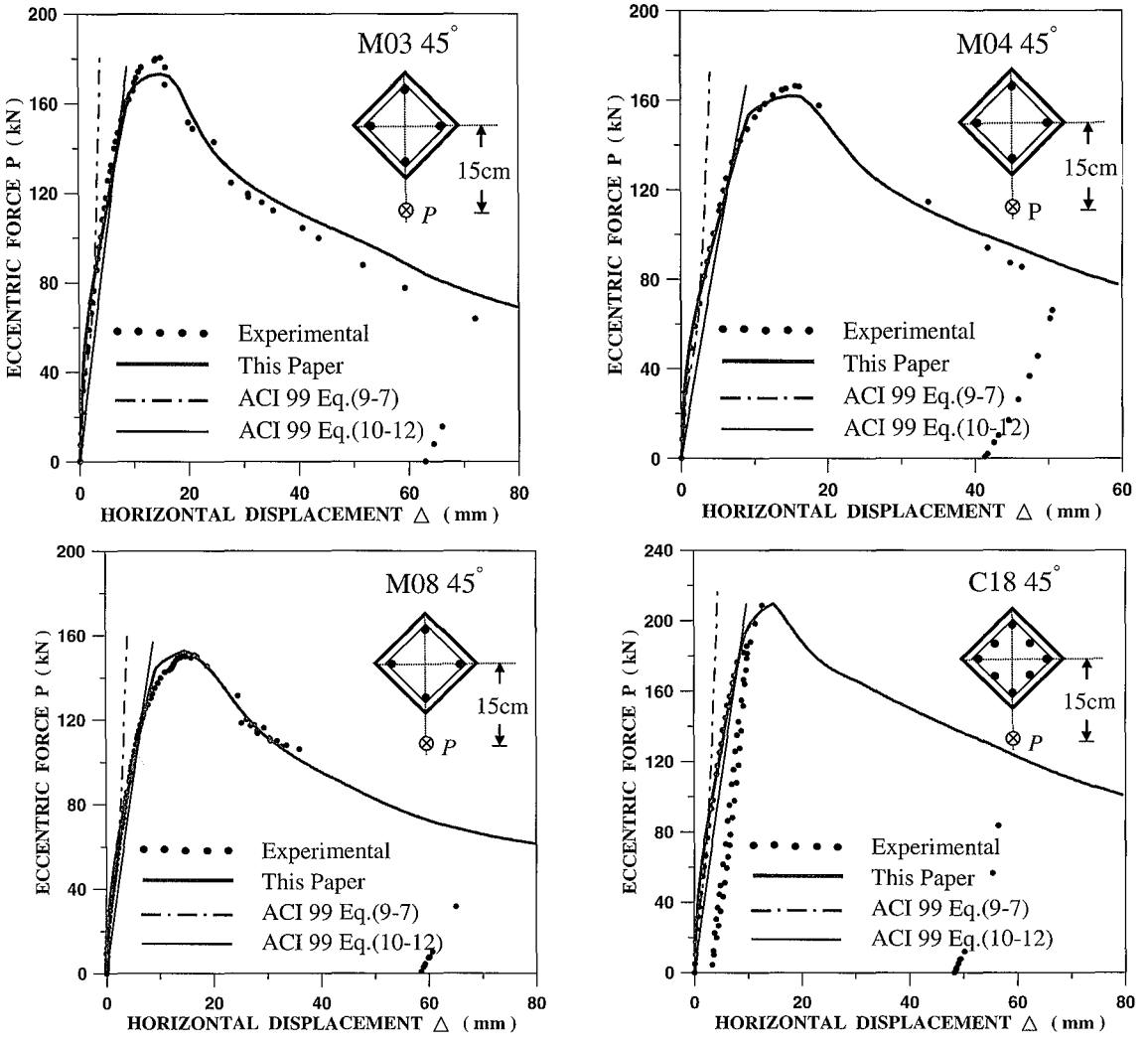

Fig. 12. Comparison of load-deflection curves (Liu, 1997)

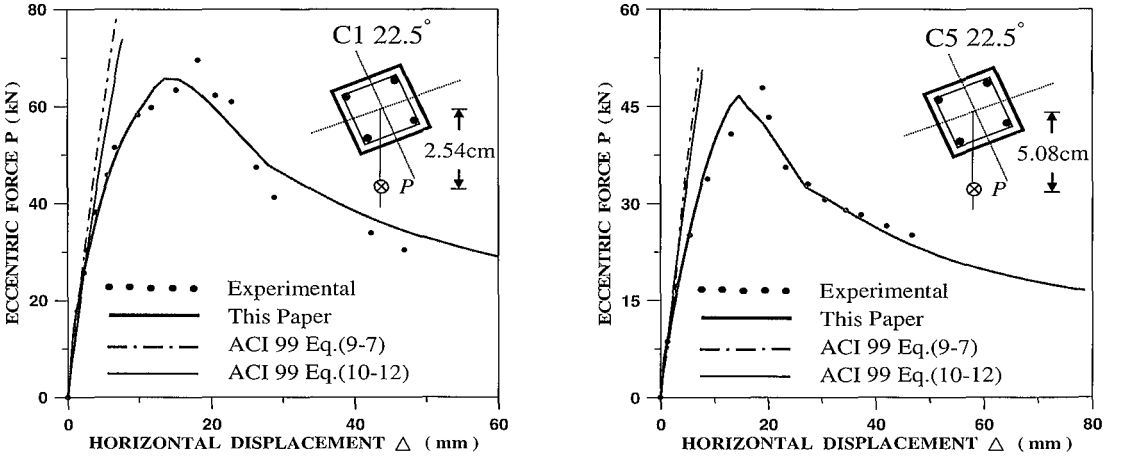

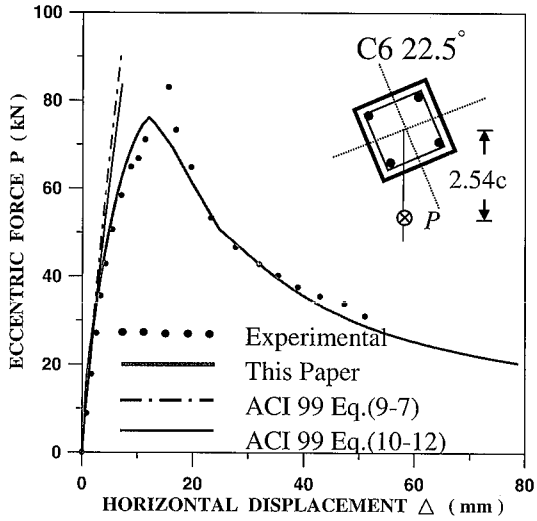

Fig. 13. Comparison of load-deflection curves (Tsao, 1991)

VII. SUMMARY AND CONCLUSIONS

1. Simply resetting the parameter values, the stress-strain equations for the material presented in this paper can be used for other material models, such as the Modified Hognestad model or parabola-rectangular model for concrete and the perfectly elastoplastic model for reinforcement.

2. This paper provides three simultaneous equations for biaxial loaded RC sections, directly derived from the equations of equilibrium and compatibility using realistic stress-strain models for concrete and reinforcement. Based on the principle of superposition, these formulas can be applied to analyze general types of column sections, such as fully-uncracked, partially-confined, channel-shaped, L-shaped and rectangular hollow-shaped cross sections.

3. The comparison between the analytical and experimental ultimate loads shows excellent agreement. The maximum and average absolute errors are 9.7% and 3.9%, respectively. The computer program developed in this paper can be used to generate three-dimensional failure surfaces, interaction diagrams and dimensionless load contours as design/check aids for sections under biaxial bending with/without an axial load. Three examples: rectangular solid, rectangular hollow, and L-shaped sections are presented. The curves are smooth enough to prove the reliability and accuracy of the algorithm presented in this paper.

4. Reasonably redefining some parameters, the effective moment of inertia I_e formula in the current *ACI* Code for flexural members can be employed to predict the load-deflection curves of RC columns under biaxial bending. In this paper, I_{cr} in the I_e formula was redefined as the moment of inertia for a cracked transformed section. The area of discrete concrete strips and reinforcement is transformed into unstressed plain concrete area using the ratio E_c^{sec}/E_c to reflect the nonlinearity of the material stress-strain curves. In the post-ultimate stage, the constant ultimate bending capacity of the column, M_u, is substituted for M_{max} to lead I_e to remain close to I_{cr}. Although the effective flexural rigidity calculation presented in this paper is simple and traditional, the experimental and analytical curves are matched excellently at

any monotonic loading stage including both the pre-ultimate and post-ultimate stages.

REFERENCES

1. ACI Committee 318, 1999, *Building Code Reqirements for Reinforced Concrete (318M-99) and Commentary (318RM-99)*, American Concrete Institude, Detroit.
2. Branson, D. E., 1977, *Deformation of Concrete Structures*, McGraw-Hill, New York, N. Y., pp. 120.
3. Branson, D. E., and Trost, H., 1982, "Application of I-Effective Method in Calculating Deflections of Partially Prestressed Concrete Members," *PCI Journal*, V. 27, No. 5, pp. 62-77.
4. Bresler, B., 1960, "Design Criteria for Reinforced Columns under Axial Load and Biaxial Bending," *ACI Journal, Proceedings* V. 57, No.5, pp. 481-490.
5. Brøndum-Nielson, T., 1997, "Serviceability Analysis of Concrete Sections under Biaxial Bending," *Journal of Structural Engineering*, V. 123, No. 1, pp.117-119.
6. Dundar, C., 1990, "Concrete Box Sections under Biaxial Bending and Axial Load," *Journal of Structural Engineering*, V. 116, No. 3, pp. 860-865.
7. Furlong, R. W., 1961, "Ultimate Strength of Square Columns under Biaxial Eccentric Loads, " *ACI Journal*, V. 57, No.9, pp. 1129-1140.
8. Furlong, R. W., 1979, "Concrete Columns under Biaxially Eccentric Thrust," *ACI Journal, Proceedings* V. 76, No.10, pp. 1093-1118.
9. Heimdahl, P. D., and Bianchini, A. C., 1975, "Ultimate Strength of Biaxially Eccentrically Loaded Concrete Columns Reinforced with High Strength Steel," *Reinforced Concrete Columns, SP-50*, American Concrete Institude, Detroit, pp. 93-117.
10. Hsu, C. T., 1974, "Behaviour of Structural Concrete Subjected to Biaxial Flexure and Axial Compression." Ph. D. Thesis, McGill University, Montreal.
11. Hsu, C. T., 1988, "Analysis and Design of Square and Rectangular Columns by Equation of Failure Surface," *ACI Structural Journal*, V. 85, No.2, pp. 167-179.
12. Krishna Mohan Rao, S.V., and Dilger, W. H., 1992, "Evaluation of Short-Term Deflection of Partially Prestressed Concrete Members," *ACI Structural Journal*, V. 89, No.1, pp. 71-78.
13. Liu, S. L., 1997, " Behavior of RC Columns under Axial Load with Bidirectional Eccentricity," Master Thesis, Department of Architecture, National Cheng Kung University, Tainan, Taiwan.
14. Park, R., and Paulay, T., 1975, *Reinforced Concrete Structures*, John Wiley and Sons, New York, N.Y., p. 56-57.
15. Park, R., Priestley, M.J.N., and Gill, W.D., 1982, " Ductility of Square-Confined Concrete Columns," *Proceedings ASCE*, Vol.108, ST4, pp. 929-950.
16. Ramamurthy, L. N., 1966, " Investigation of the Ultimate Strength of Square and Rectangular Columns under Biaxially Eccentric Loads," *Symposium on Reinforced Concrete Columns, SP-13*, American Concrete Institute, Detroit, pp. 263-298.
17. Resheidat, M., Ghanma, M., Sutton C., and Chen, W. F., 1996, "Flexural Rigidity of Biaxially Loaded RC Rectangular Column Sections, " *Journal of Strctrual Engineering*, V. 22, No. 4, pp. 201-210.

18. Rodriguez, J. A., and Aristizabal-Ochoa, J. D., 1999, " Biaxial Interaction Diagrams for Short RC Columns of Any Cross Section," *Journal of Structural Engineering*, V. 125, No. 6, pp. 627-683.
19. Sakai, K., and Kakuta, Y., 1980, "Moment-Curvature Relationships of Reinforced Concrete Members Subjected to Combined Bending and Axial Force," *ACI Journal*, Proceeding V.77, No.3, pp. 189-194.
20. Taylor, M. A., 1985, "Direct Biaxial Design of Columns," *Journal of Strctrual Engineering*, V. 111, No. 1, pp. 158-173.
21. Tsao, W. H., 1991, "Behavior of Square and L-shaped RC Columns under Combined Biaxial Bending and Axial Compression," Ph. D. Thesis, New Jersey Institude of Technology.
22. Wang, G. G., and Hsu, C. T., 1992, "Complete Biaxial Load-Deformation Behavior of RC Columns," *Journal of Structural Engineering*, V.118, No. 9, pp. 2590-2609.
23. Wenger, R., 1978, "Finite Element Models for Reinforced Concrete," *Formulations and Computational Algorithms in Finite Element Analysis*, edited by Bathe, K. J., Oden, J. T., and Wunderlich, W., M.I.T, America, pp. 393-439.
24. William, H. P., Saul, A. T., William, T. V., and Brian, P. P., 1994, *Numerical Receipes in Fortran* 2nd, Cambridge University Press, pp. 347-383.
25. Yen, R. J., 1991, " Quasi-Newton Method for Reinforced-Concrete Column Analysis and Design," *Journal of Structural Engineering*, V. 117, No. 3, pp. 657-666.